A study of exchange interaction in Cr^{3+}-doped $CaY_{1-x}Gd_xAlO_4$

1997 J. Phys.: Condens. Matter 9 1575

(http://iopscience.iop.org/0953-8984/9/7/019)

J. Phys.: Condens. Matter **9** (1997) 1575–1584. Printed in the UK PII: S0953-8984(97)77963-3

A study of exchange interaction in Cr^{3+}-doped $CaY_{1-x}Gd_xAlO_4$

M Yamaga†, P I Macfarlane‡, Keith Holliday‡, B Henderson‡, N Kodama§ and Y Inoue¶

† Department of Electronics, Faculty of Engineering, Gifu University, Gifu 501-11, Japan
‡ Department of Physics and Applied Physics, University of Strathclyde, Glasgow G1 1XN, UK
§ Department of Chemistry, Faculty of Education, Akita University, Akita 010, Japan
¶ Tosoh Corporation, Ayase 120, Japan

Received 19 September 1996, in final form 9 December 1996

Abstract. The broadening of the R_1 lines of Cr^{3+} impurity ions in the substitutionally disordered crystals $CaY_{1-x}Gd_xAlO_4$ ($x = 0, 0.1, 0.5, 1$) has been studied. Fluorescence line narrowing removes the inhomogeneous broadening created by variation in the crystal field and results in instrument-limited spectral features for $x = 0$ and 0.1. Exchange interactions between Cr^{3+} ions in octahedral positions and Gd^{3+} ions at second-nearest-neighbour sites cause significant broadening of the narrowed R_1 line when $x = 0.5$ and 1. Comparisons of experimental and simulated spectra have been used to estimate the magnitude of the exchange-coupling constant, $J \simeq 2$–$3\ cm^{-1}$. Such simulations also show that the selection rule for the $^2E \rightarrow {}^4A_2$ transition is broken by the Gd^{3+} spin in the Cr^{3+}–Gd^{3+} exchange system.

1. Introduction

$CaYAlO_4$ (CYA) is a crystal with the K_2NiF_4 structure having space group $I4/mmm$ (D_{4h}^{17}) [1]. Cr^{3+} ions preferentially occupy the Al^{3+} sites, which are octahedrally coordinated to six nearest-neighbour O^{2-} ions with eight second-neighbour sites occupied by Ca^{2+} and Y^{3+} ions. The Ca^{2+} and Y^{3+} ions randomly occupy these sites such that the overall crystal stoichiometry is maintained. The substitutional disorder of Ca^{2+} and Y^{3+} ions in CYA produces an energy distribution of the ground and excited states of Cr^{3+} ions which causes the inhomogeneous broadening of the optical and ESR spectra [2, 3].

The random occupation of the nearest cation shell by Ca^{2+} and Y^{3+} ions causes displacements of the octahedron of nearest-neighbour oxygen ions. The symmetry at the Al^{3+} sites is consequently tetragonally distorted, the magnitude of the distortion varying from site to site. Such distortions lift the degeneracies of the different energy levels of Cr^{3+} ions substituted at the Al^{3+} site, resulting in shifts and splittings of their observed spectra. The splitting of the $^4A_2$ ground state by the tetragonal distortion is too small to be measured by conventional optical spectroscopy but may be resolved by fluorescence line-narrowing (FLN) and electron spin-resonance (ESR) spectroscopies [2, 3]. The ^2E state splits into ^2Eu and ^2Ev states, with ^2Eu lying lowest by virtue of the stretched distortion [1]. The consequence is that the R-line spectrum ($^2E \rightarrow {}^4A_2$) splits into R_1 ($^2Eu \rightarrow {}^4A_2$) and R_2 ($^2Ev \rightarrow {}^4A_2$) lines with R_2 occurring at a shorter wavelength than R_1 [4, 5]; its effects are easily recognizable in the excitation of FLN spectra [2].

0953-8984/97/071575+10$19.50

A previous study of Cr^{3+}:CYA showed the broadening of the optical $^2E \rightarrow {}^4A_2$ transitions to be dominated by variations in the non-octahedral contribution to the crystal field [2]. Taking into account the FLN results, the ESR spectra were interpreted in terms of a model of the local configurations consisting of the octahedral sites and the randomly occupied Ca^{2+}/Y^{3+} second-nearest-neighbour ions, which is based on the tilting of the principal ζ-axis of the Cr^{3+} ion from the crystalline c-axis [3]. This model is deduced from the symmetry of the various Cr^{3+} sites. Further experimental information on the microstructure of the Cr^{3+} environment is required to provide a realistic distribution of Ca^{2+} and Y^{3+} ions in CYA.

The broadening of the R_1 line of Cr^{3+} in Gd-based oxides by exchange interaction between Cr^{3+} and Gd^{3+} ions has been reported by Murphy and Ohlmann [6], Monteil *et al* [7, 8], and Yamaga *et al* [9, 10]. The width of the R_1 line depends strongly on the strength of the exchange interaction and the number of Gd^{3+} ions in near-neighbour sites. In consequence, the combined spin of the exchange-coupled Cr^{3+}–Gd^{3+} system may be used to probe the local environment in disordered crystals. $CaY_{1-x}Gd_xAlO_4$ (CYGA) crystals ($x = 0$, 0.1, 0.5, 1) have been grown to further examine the microstructure of the substitutional disorder in this family of crystals. In this way, the number of nearby Gd^{3+} ions increases with x and the influence on the broadening can be measured. This paper reports an experimental study of the broadening of the R_1 line in CYGA crystals which is analysed in terms of the Cr^{3+}–Gd^{3+} exchange interaction as it varies as a function of x.

2. Experimental results

The details of the crystal growth of CYA and the experimental techniques used to obtain the FLN spectra were described in reference [2]. The concentration of Cr^{3+} ions in CYGA was 0.5 at.%. The FLN spectra of the R_1 line of Cr^{3+} in CYGA were measured at 14 K.

Figure 1 summarizes the FLN data for the samples with $x > 0$, showing for each sample both resonant and non-resonant spectra, the latter being the lowest of each series. The non-resonant spectra do not represent the fluorescence of all Cr^{3+} ions as selection takes place even when exciting into the broad absorption bands at much higher photon energy [2]. Spectra shown for excitation to the ^2E (^2Eu, ^2Ev) and to the $^4T_2$ band are shown for different samples. In the two cases the lines have similar widths though the peaks shift with differing excitation energies, both between samples and for the same sample.

Figure 1(a) shows the FLN spectra measured for the crystal with composition $CaY_{0.9}Gd_{0.1}AlO_4$. The peak energy of the FLN spectrum is coincident with the excitation energy, but there are also features to the lower- and higher-energy sides of the sharp line. The width of the broad line is about 30 cm^{-1}, and its intensity increases as the excitation energy decreases. This broad feature is not present in the resonant FLN spectrum of pure CYA [2] and the tails distributed on the lower- and higher-energy sides of the excitation energy shown in figure 1(a) are attributed to the effects of Gd^{3+} ions in the CYGA crystal.

Figure 1(b) shows the FLN spectra measured for a crystal of composition $CaY_{0.5}Gd_{0.5}AlO_4$. The FLN spectrum excited at 13 382 cm^{-1} has no sharp resonant line as was observed for CYA [2] and $CaY_{0.9}Gd_{0.1}AlO_4$. The peak energy of the FLN spectrum is shifted to lower energy from the excitation energy, and the linewidth ($\simeq$70 cm^{-1}) is large, although it is smaller than that (110 cm^{-1}) obtained for non-resonant excitation. This behaviour is similar to that observed for Cr^{3+}:$Gd_3Sc_2Al_3O_{12}$ (GSAG), where the broadening is caused by exchange interaction between the spins of Cr^{3+} and six equivalent second-nearest-neighbour Gd^{3+} ions [9, 10]. The FLN spectrum recorded with 13 443 cm^{-1} excitation is somewhat different: a second, weaker peak appears, shifted to lower energy.

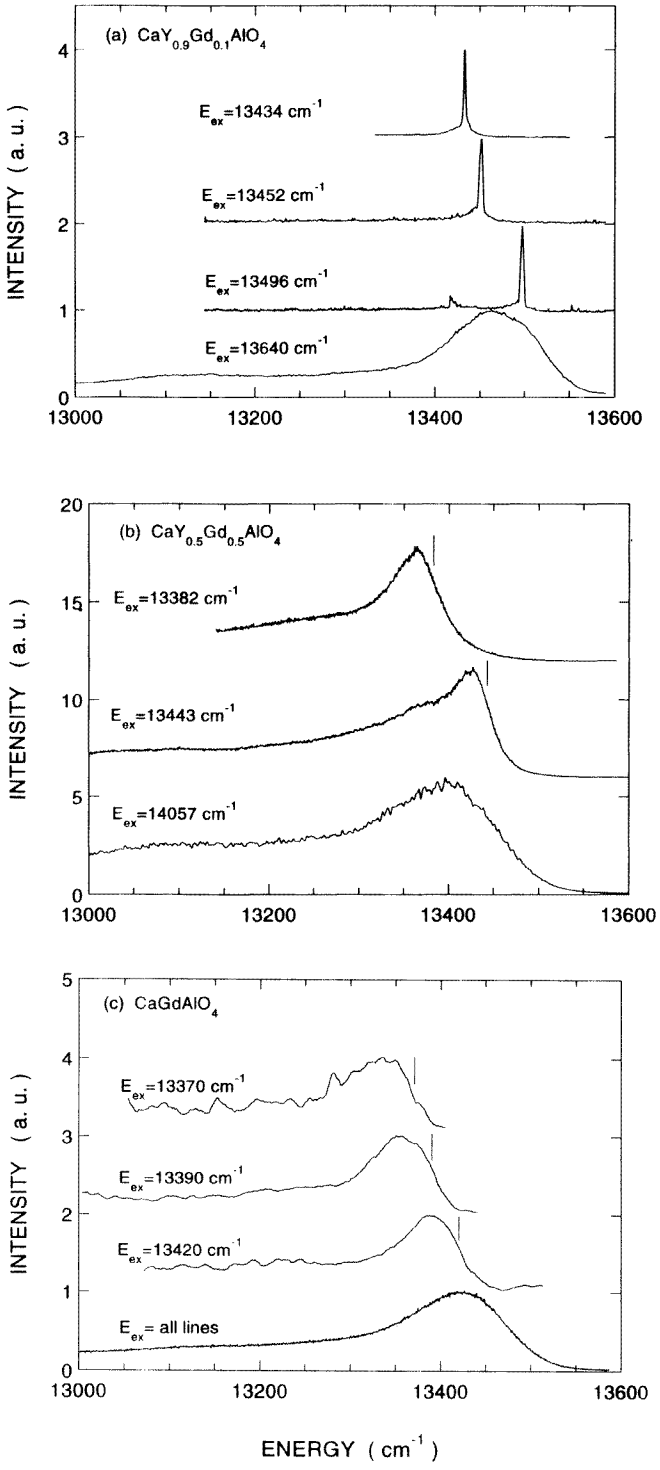

Figure 1. FLN spectra of Cr^{3+} in $CaY_{1-x}Gd_xAlO_4$ for (a) $x = 0.1$, (b) $x = 0.5$, and (c) $x = 1$. The bars in (b) and (c) show laser excitation energies. All lines in (c) means all lines emitted from an Ar^+-ion laser.

This feature is attributed to excitation resonant with the low-energy wing of the R_2 line which fluorescences via the R_1 line: that is, the line consists of both resonant and non-resonant components [2].

Figure 1(c) shows the FLN spectra of Cr^{3+} ions in $CaGdAlO_4$ (CGA). The peak energies of the broad FLN spectra are shifted from the excitation energy towards lower energy as the excitation energy decreases. The width ($\sim$80 cm^{-1}) is slightly larger than that ($\sim$70 cm^{-1}) in $CaY_{0.5}Gd_{0.5}AlO_4$.

3. Discussion

3.1. The spin Hamiltonian of Cr^{3+}

The spin Hamiltonian of Cr^{3+} in CYGA crystals is given by

$$\mathcal{H} = \lambda \boldsymbol{L}_{\mathrm{Cr}} \cdot \boldsymbol{S}_{\mathrm{Cr}} + (-J)\boldsymbol{S}_{\mathrm{Cr}} \cdot \boldsymbol{S}. \tag{1}$$

The first term is the spin–orbit interaction, where $\boldsymbol{L}_{\mathrm{Cr}}$ and $\boldsymbol{S}_{\mathrm{Cr}}$ are fictitious angular and spin momenta of Cr^{3+}, and λ is the effective spin–orbit-coupling constant. The spin–orbit interaction mixes the $^4T_2$ excited state into the ^2E excited state and allows the spin-forbidden transition to the ground state, $^2E \rightarrow {}^4A_2$ [4, 5]. The magnitude of λ is about 100 cm^{-1} [2, 3]. The second term in equation (1) is the exchange interaction between the spins of Cr^{3+} and the second-nearest-neighbour Gd^{3+} ions, assumed to be isotropic and ferromagnetic (J is positive). The spin of Cr^{3+} in the $^4A_2$ ground state is $S_{\mathrm{Cr}} = 3/2$ and $S_{\mathrm{Cr}} = 1/2$ in the ^2E excited state. The total spin of n interacting Gd^{3+} ions is $\boldsymbol{S} = \sum_{i=1}^{n} \boldsymbol{S}_i$ where $\boldsymbol{S}_i$ is the spin of the ith Gd ion. If the exchange constant J is small, each of the $M_s = 3/2$, 1/2, $-1/2$, $-3/2$ levels of the $S_{\mathrm{Cr}} = 3/2$ ground state is split into a quasi-continuous band of exchange-coupled sub-levels having total spin quantum numbers $\tilde{S}$ given by $\tilde{S} = S + 3/2$, $\tilde{S} = S + 1/2$, $\tilde{S} = |S - 1/2|$, $\tilde{S} = |S - 3/2|$ [6]. In CYGA, the ^2E state is split by the spin–orbit coupling and axial distortion into ^2Eu and ^2Ev states, the observed separation in CYA being 160 cm^{-1} [2]. The lower ^2Eu level consists of two sub-bands, one corresponding to $\tilde{S} = S + 1/2$ and the other to $\tilde{S} = |S - 1/2|$. The exchange-interaction Hamiltonian (H_{ex}) is diagonal in $\tilde{S}$, $M_{\tilde{S}}$, S and S_{Cr} [6, 9, 10]. The expectation value of H_{ex} for states defined by the quantum numbers $\tilde{S}$, $M_{\tilde{S}}$, S, S_{Cr} is given by

$$\langle \tilde{S}, M_{\tilde{S}}, S, S_{\mathrm{Cr}} | H_{\mathrm{ex}} | \tilde{S}, M_{\tilde{S}}, S, S_{\mathrm{Cr}} \rangle = -\frac{J}{2}[\tilde{S}(\tilde{S}+1) - S(S+1) - S_{\mathrm{Cr}}(S_{\mathrm{Cr}}+1)] \tag{2}$$

and is independent of $M_{\tilde{S}}$. Figure 2 shows the electron spin density of the $S_{\mathrm{Cr}} = 3/2$ ground state (using J as an energy unit) split by exchange interactions, H_{ex}, for one Gd^{3+} ion ($n = 1$), two equivalent Gd^{3+} ions ($n = 2$), and four equivalent Gd^{3+} ions ($n = 4$), respectively. The bars in figure 2 indicate the degeneracy of the spin states with total spins $\tilde{S}$ and S, defined as $(2\tilde{S}+1)N_S$. N_S is the total number of ways of forming a state of total spin $\boldsymbol{S}$ of Gd^{3+}, where the values of N_S for $n = 1$ and 2 are equal to 1. N_S for $n = 4$ is calculated in the same way as by Murphy and Ohlmann [6] and its values are listed in table 1.

3.2. Calculating the FLN line shape

If the energy distributions in the ground and excited states of an optical transition are determined only by variations in the strength of the local crystal field, then FLN techniques are able to measure the homogeneous linewidth when this is greater than the experimental resolution. This is usually less than 0.1 cm^{-1} for the R lines in Cr^{3+}-doped crystals at low

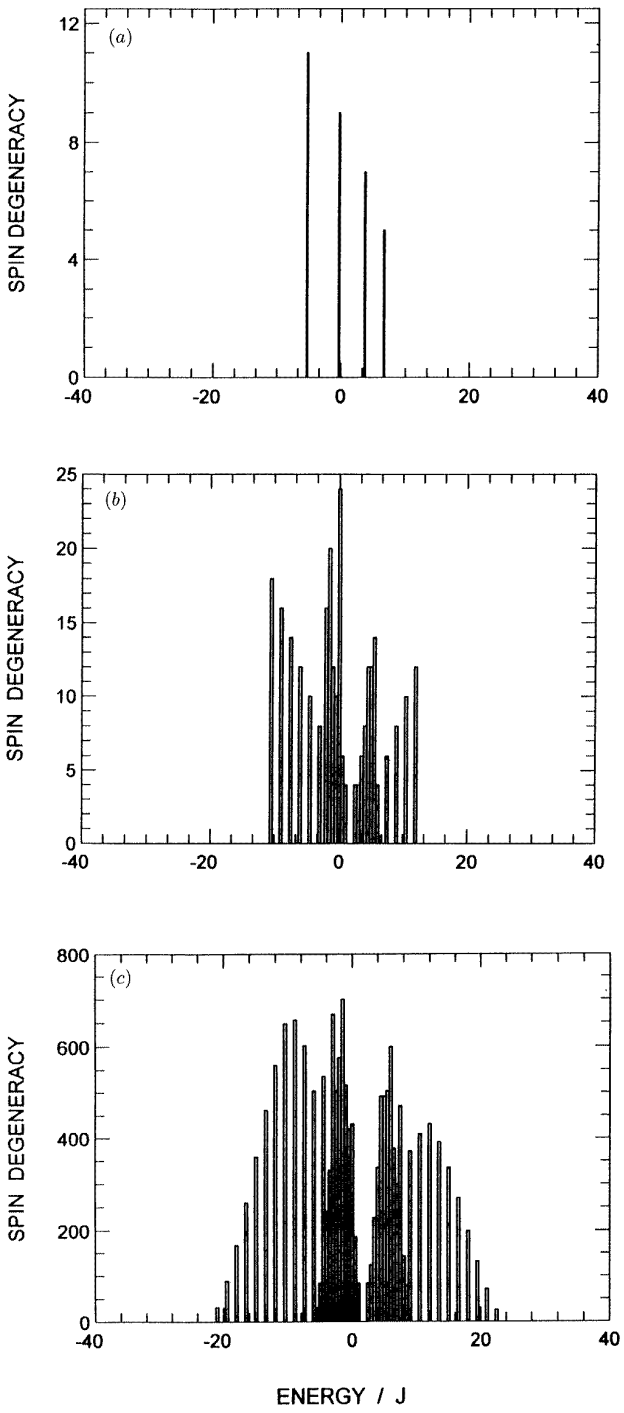

Figure 2. The spin degeneracy of the ground state with J as the energy unit, split by exchange interaction of Cr^{3+} with (a) one Gd^{3+} ion, (b) two equivalent Gd^{3+} ions, and (c) four equivalent Gd^{3+} ions.

Table 1. The total number of vectors of length S formed by adding together four vectors of length 7/2.

S	0	1	2	3	4	5	6	7	8	9	10	11	12	13	14
N_S	8	21	31	38	42	43	41	36	28	21	15	10	6	3	1

temperatures [2, 7–9]. However, as shown in figure 2, the ground state of a single Cr^{3+} ion is split into four quasi-continuous bands by exchange between Cr^{3+} and the surrounding Gd^{3+} ions, and the ^{2}Eu excited state, which emits as the R_1 line, splits into two quasi-continuous bands. Resonant excitation of the R_1 line excites transitions into these ^{2}Eu energy levels, interacting with a subset of ions determined by the disorder and the two quasi-continuous bands of the spin state. The linewidths of the FLN lines of Cr^{3+}-doped CYGA crystals are broadened by the exchange interaction between Cr^{3+} ions and nearest-neighbour Gd^{3+} ions. The shape of the FLN line reflects the quasi-continuous bands of both excited- and ground-state spins. The magnitude of the exchange constant is estimated by simulating the narrowed line shape for comparison with the experimental spectra [9, 10].

The line shape of the resonant FLN spectrum is calculated by assuming that the distribution function, $P_{\rm dis}(\omega)$, for the strength of the crystal field at the ^{2}Eu excited state is given by a Gaussian function:

$$P_{\rm dis}(\omega) = \frac{1}{\sqrt{2\pi}\gamma} \exp\left(- \frac{(\omega - \omega_1)^2}{2\gamma^2} \right) \tag{3}$$

where ω_1 is the energy of the ^{2}Eu excited state of maximum probability and γ is the width. The electron spin density of the ^{2}Eu state, $P^E_{\rm spin}(E)$, is given by $(2\tilde{S}+1)N_S$ with energy, E, corresponding to the diagonal element in equation (2). The energy distribution of the ^{2}Eu state is therefore given by the convolution:

$$P_{\rm Eu}(\omega) = \int_0^\infty P_{\rm dis}(E) P^E_{\rm spin}(\omega - E)\ {\rm d}E. \tag{4}$$

We assume that Cr^{3+} ions excited into the ^{2}Eu level by resonant laser excitation, $E_{\rm ex}$, relax to their lowest excited spin level at $T = 0$ K without energy transfer between Cr^{3+} sites. The distribution, $P_{\rm abs}(E)$, of excited Cr^{3+} sites occupied at the lowest excited spin level is proportional to $P_{\rm dis}(E)P^E_{\rm spin}(E_{\rm ex} - E)$, represented by a discrete function which is calculated numerically. The line shape of intrinsic R_1-line luminescence from a single Cr^{3+} site, $P_{\rm em}(E)$, is given by modifying the quasi-continuous bands, $P^G_{\rm spin}(E)$, of the ground spin state, and applying the spin-selection rule of the Cr^{3+} $\pm 1/2 \leftrightarrow \mp 3/2$ transitions [4, 5] and of Gd^{3+} spins in the Cr^{3+}–Gd^{3+} exchange system [6]. The calculated FLN line shape including the resonant excitation and emission processes is the convolution of the distribution function of the excited Cr^{3+} sites and the intrinsic luminescence line shape, i.e.

$$I(E) = \int_0^\infty P_{\rm abs}(E') P_{\rm em}(E - E')\ {\rm d}E'. \tag{5}$$

3.3. Simulation of the FLN spectra

The peak energy of the FLN spectra in $CaY_{1-x}Gd_xAlO_4$ ($x = 0.1$, 0.5, 1) is shifted to lower energy from the excitation energy and the asymmetric line shape has a pronounced low-energy tail. The linewidths of the FLN spectra increase as the concentration of Gd^{3+}

ions, x, increases. In order to explain these results, we have calculated the line shapes of the FLN spectra of Cr^{3+} in the exchange-coupled system by varying J as a free parameter.

First, the FLN line shape of a Cr^{3+} ion interacting with a single Gd^{3+} ion in $CaY_{0.9}Gd_{0.1}AlO_4$ is calculated. The $^4A_2$ ground state is split into four spin levels defined as $|5, M_{\tilde{S}}, 7/2, 3/2\rangle$, $|4, M_{\tilde{S}}, 7/2, 3/2\rangle$, $|3, M_{\tilde{S}}, 7/2, 3/2\rangle$, and $|2, M_{\tilde{S}}, 7/2, 3/2\rangle$, whereas ^{2}Eu splits into two spin levels, $|4, M_{\tilde{S}}, 7/2, 1/2\rangle$ and $|3, M_{\tilde{S}}, 7/2, 1/2\rangle$. The lowest ground and excited spin states are $|5, M_{\tilde{S}}, 7/2, 3/2\rangle$ and $|4, M_{\tilde{S}}, 7/2, 1/2\rangle$, respectively, assuming that $J > 0$. As the spin states are characterized by total spin $\tilde{S}$, the spin state is simply denoted by the value of $\tilde{S}$. The transitions from the lowest spin level of the ^{2}Eu excited state with $\tilde{S} = 4$ to the $^4A_2$ ground spin levels with $\tilde{S} = 5$, 4, 3 are allowed through spin–orbit interaction. Although the transition to the spin state with $\tilde{S} = 2$ is still spin forbidden, the transition strength may not be negligible. The probabilities of transitions to the states with $\tilde{S} = 5$, 4, 3, 2 are defined as R_1, R_2, R_3, and R_4, respectively.

At $T = 0$ K, electrons occupy the lowest spin level of the ground state. The laser excitation excites two Cr^{3+} sites with different crystal fields and total spins $\tilde{S} = 4$ and $\tilde{S} = 3$ in $CaY_{0.9}Gd_{0.1}AlO_4$. Electrons excited into the $\tilde{S} = 3$ spin state relax to the lowest excited spin state with $\tilde{S} = 4$ without energy transfer to other sites. The calculated FLN spectrum is composed of the luminescence from the two Cr^{3+} sites with slightly different crystal fields. The bars in the lower part of figure 3(a) are calculated using equation (5), with R_1:R_2:R_3:R_4 = 1:0.5:0.5:0.2, $J = 2$ cm^{-1} and $T = 14$ K. The ratio is consistent with parameters that have been shown to be realistic in similar systems [8, 9]. The calculation includes thermal distributions of electrons in the ground- and excited-state spin levels. The only free fitting parameter is J. The solid curve is the envelope assuming that each bar has a width of $\gamma_0 = 5$ cm^{-1}. The peak of the calculated curve is seen to be shifted from the resonant excitation energy, in agreement with the experimentally obtained spectra in the upper part of figure 3(a). The tail at higher energy is due to the Boltzmann distribution at 14 K. The sharp feature that dominates the spectra in figure 3(a) is attributed to Cr ions that have no Gd ions in the nearest-neighbour cation shell and is therefore resolution limited as in CYA [2].

The number of Gd^{3+} ions in the neighbourhood of Cr^{3+} ions increases as the Gd^{3+} concentration increases. For crystals with composition $CaY_{0.5}Gd_{0.5}AlO_4$, the most probable configuration is that for which there are four Ca^{2+}, two Y^{3+} and two Gd^{3+} ions occupying the eight second-nearest-neighbour sites. Two nearby Gd^{3+} ions produce a much wider energy distribution of the spin levels of the ground and excited states of Cr^{3+} than a single Gd^{3+} ion, as shown in figure 1. The asymmetric and broadened FLN spectra observed in $CaY_{0.5}Gd_{0.5}AlO_4$ can be explained by the presence of more than one Gd^{3+} ion. The line shape of the FLN spectrum of Cr^{3+} is calculated using the same parameters as for $x = 0.1$ assuming that Cr^{3+} ions interact with two equivalent Gd^{3+} ions. Again, J is a free parameter and a value of 3 cm^{-1} is optimum. The results are shown in the lower part of figure 3(b) to give a good fit. The discrepancy at lower energy is due to the overlap of the R_1 line and the one-phonon sideband observed experimentally at 14 K. In the same way, the line shape of the FLN spectrum of Cr^{3+} interacting with four equivalent Gd^{3+} ions is calculated and shown in the lower part of figure 3(c). Good agreement with the experimental FLN spectrum for Cr^{3+}:CGA is observed.

3.4. A model of the ionic configuration

The $3d^3$ ion, Cr^{3+}, preferentially substitutes at octahedral Al^{3+} sites, which have six nearest-neighbour O^{2-} ions and eight second-neighbour sites randomly containing Ca^{2+} and Y^{3+}

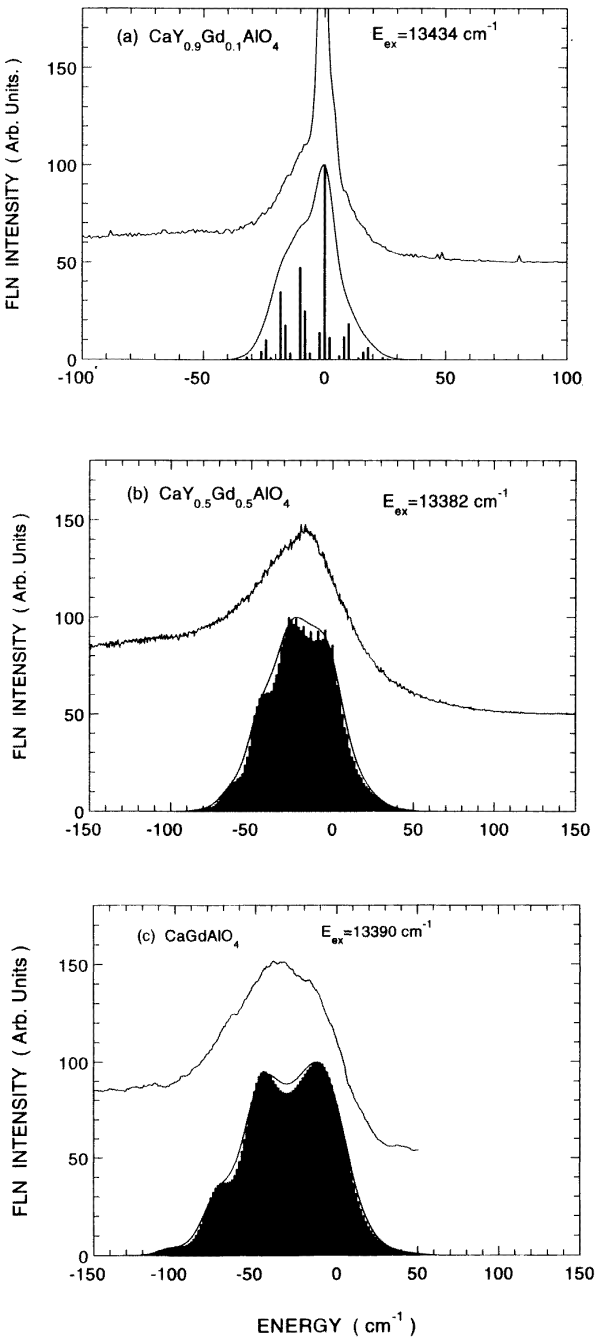

Figure 3. The upper curves are the observed FLN spectra of Cr^{3+} in $CaY_{1-x}Gd_xAlO_4$ for (a) $x = 0.1$, (b) $x = 0.5$, and (c) $x = 1$. The bars in the lower parts of the figures were calculated using equation (5), the intensity ratio $R_1{:}R_2{:}R_3{:}R_4 = 1{:}0.5{:}0.5{:}0.2$, temperature $T = 14$ K, and the exchange-coupling constants $J = 2$ cm^{-1} and $J = 3$ cm^{-1}, respectively, for $x = 0.1$ and $x = 0.5$, 1. The solid curves are the envelopes assuming that each bar has a width of $\gamma_0 = 5$ cm^{-1}. The origin of energy is equal to the excitation energy.

ions. The statistical probabilities of $8-n$ Ca^{2+} and n Y^{3+} ions constituting the nearest cation shell at any given Cr^{3+} site are given by ${}_8C_n$. However, the ESR data for Cr^{3+}:CYA [3] confirm that there are no detectable sites with configurations that result in a large mismatch in the local charge balance, i.e. when $n \leqslant 2$ or $n \geqslant 6$. The most probable configuration consists of four Ca^{2+} and four Y^{3+} ions, there being several different rearrangements of Ca^{2+} and Y^{3+} for this ratio [3].

The ESR spectra of Gd^{3+} are broadened by the spin–spin interaction so strongly as to render different sites inseparable from one another. It is therefore necessary to apply the model developed for CYA to the FLN spectra of the mixed systems in order to see whether the model still applies. First consider the case of $CaY_{0.9}Gd_{0.1}AlO_4$. The sharp and broadened FLN lines coexist for excitation energies in the range 13 400–13 530 cm^{-1}. The appearance of both contributions in the FLN spectra throughout the R_1 line implies that the energy difference between the two configurations with Gd^{3+} ions and without Gd^{3+} ions is small compared to the width of the distribution function caused by disorder. This is not unexpected as the R lines in even the most extreme comparison of CYA and CGA appear at almost the same wavelengths. These results also suggest that the inhomogeneous broadening is caused both by disorder among the eight second-nearest-neighbour cations, and the more remote third- and fourth-nearest-neighbour cations. However, Cr^{3+} ions may interact with one Gd^{3+} ion in the next-nearest-neighbour site because the exchange interaction is a rapidly decreasing function of the increasing separation between Cr^{3+} and Gd^{3+} ions.

The linewidths of the FLN spectra of Cr^{3+} in $CaY_{0.5}Gd_{0.5}AlO_4$ and CGA are very similar over the whole range of excitation energies, and the FLN spectra of both crystals calculated using $J = 3$ cm^{-1} and the transition probabilities obtained from the $CaY_{0.9}Gd_{0.1}AlO_4$ results fit the observed FLN spectra. At a glance these results indicate that the dominant configuration keeps the charge balance of the second-nearest-neighbour Ca^{2+}, $1-x$ Y^{3+}, and x Gd^{3+} ions in $CaY_{1-x}Gd_xAlO_4$. However, it may seem physically unrealistic that the best fits to the data for crystals of different x require different values of J. This is easily explained as being a consequence of modelling each crystal as being a single configuration of nearest neighbours. In the case of $x = 0.1$ this is quite reasonable. There will be very few Cr^{3+} ions that have more than one Gd^{3+} nearest neighbour. In the case of $x = 0.5$, only a configuration containing two Gd^{3+} ions is considered. Whilst this is the most likely configuration, there will also be Cr^{3+} ions that have three or four Gd^{3+} neighbours in the nearest cation shell and these will cause further broadening of the FLN features. Similarly, when $x = 1$, only the configuration consisting of four Gd^{3+} ions is used despite the fact that configurations of five or six Gd^{3+} ions will cause further broadening. A value of $J = 2$ cm^{-1}, obtained for $x = 0.1$, is therefore the most physically realistic though it is possible that this value may vary a little with x as the lattice constant varies. A value of 3 cm^{-1} is, however, an overestimate caused by neglecting the contributions of minority configurations.

4. Conclusions

The R_1 line of Cr^{3+} in CYGA crystals is broadened by several mechanisms. The FLN spectra reflect broadening processes associated with exchange interaction between the Cr^{3+} and Gd^{3+} ions in CYGA. Simulating the FLN spectra of Cr^{3+}:CYGA has allowed an estimate of the exchange energy of $J \simeq 2$–3 cm^{-1} to be made. Although the selection rule for the ${}^2E \rightarrow {}^4A_2$ transition dictates that the Gd^{3+} spins in the Cr^{3+}–Gd^{3+} exchange system must be conserved, the simulated FLN line shapes indicate that the selection rule for the Gd^{3+} spin is lifted in zero magnetic field.

The FLN simulations have also allowed the substitutional disorder in the crystals to be investigated. It appears that the dominant configuration in $CaY_{1-x}Gd_xAlO_4$ maintains charge balance, such that eight second-nearest-neighbour cations are composed of 4 Ca^{2+} ions, $4(1-x)$ Y^{3+} ions, and $4x$ Gd^{3+} ions. There are some indications that the mixing of Y and Gd ions may be somewhat freer than determined by this expression. This is reasonable given the fact that the charges on these ions are equivalent, so their interchange does not influence local charge balance.

Acknowledgments

This work was supported through a Grant-in-Aid for Scientific Research on the Priority Area 'New Development of Rare Earth Complexes' (No 07230233, 08220228) and on Fundamental Research (No 07650049) from the Ministry of Education, Science and Culture and joint research (1995–1996) between the Japan Society for the Promotion of Science and the Royal Society/British Council. At Strathclyde, the research programme was funded by joint EPSRC/MOD research grants (GR/F/54105 and GR/H/66143) and the Nuffield Foundation.

References

[1] Shannon R D, Oswald R A, Parise J B, Chai B H T, Byszowski P, Pajaczow A and Sobolewski R 1992 *J. Solid State Chem.* **98** 90
[2] Yamaga M, Macfarlane P I, Holliday K, Henderson B, Kodama N and Inoue Y 1996 *J. Phys.: Condens. Matter* **8** 3487
[3] Yamaga M, Yosida T, Fukui M, Takeuchi H, Kodama N, Inoue Y, Macfarlane P I, Holliday K and Henderson B 1996 *J. Phys.: Condens. Matter* **8** 10 633
[4] Henderson B and Imbusch G F 1989 *Optical Spectroscopy of Inorganic Solids* (Oxford: Oxford University Press) ch 4
[5] Sugano S, Tanabe Y and Kamimura H 1970 *Multiplets of Transition Metal Ions in Crystals* (New York: Academic)
[6] Murphy J and Ohlmann R C 1967 *Optical Properties of Ions in Crystals* ed H M Crosswhite and H W Moos (New York: Wiley) pp 239–50
[7] Monteil A 1990 *J. Phys.: Condens. Matter* **2** 9639
[8] Monteil A, Ferrari M and Rossi F 1991 *Phys. Rev.* B **43** 3646
[9] Gao Y, Yamaga M, Ogihara C, O'Donnell K P and Henderson B 1992 *J. Phys.: Condens. Matter* **4** 7307
[10] Yamaga M, Gao Y, O'Donnell K P and Henderson B 1992 *J. Phys.: Condens. Matter* **5** 915